Applied Materials Today 26 (2022) 101394

Contents lists available at ScienceDirect

Applied Materials Today

journal homepage: www.elsevier.com/locate/apmt

Progress and perspective on different strategies to achieve wake-up-free ferroelectric hafnia and zirconia-based thin films

J.P.B. Silva [a,*], K.C. Sekhar [b], R.F. Negrea [c,d], J.L. MacManus-Driscoll [e,*], L. Pintilie [c]

[a] Centre of Physics of University of Minho and Porto (CF-UM-UP), Campus de Gualtar, 4710-057 Braga, Portugal
[b] Department of Physics, School of Basic and Applied Science, Central University of Tamil Nadu, Thiruvarur 610 101, India
[c] National Institute of Materials Physics, 105 bis Atomistilor, 077125 Magurele, Romania
[d] BCAST, Brunel University London, Uxbridge, Middlesex UB8 3PH, U.K.
[e] Dept. of Materials Science and Metallurgy, 27 Charles Babbage Rd., Cambridge, CB3 OFS, U.K.

ARTICLE INFO

Article history:
Received 24 November 2021
Revised 7 January 2022
Accepted 18 January 2022

Keywords:
(Pseudo-)binary oxides
Ferroelectricity
Wake-up effect
Epitaxial growth

ABSTRACT

In the last decade orthorhombic hafnia and zirconia films have attracted tremendous attention arising from the discovery of ferroelectricity at the nanoscale. However, an initial wake-up pre-cycling is usually needed to achieve a ferroelectric behaviour in these films. Recently, different strategies, such as microstructure tailoring, defect, bulk and interface engineering, doping, NH_3 plasma treatment and epitaxial growth, have been employed to obtain wake-up free orthorhombic ferroelectric hafnia and zirconia films. In this work we review recent developments in obtaining polar hafnia and zirconia-based thin films without the need of any wake-up cycling. In particular, we discuss the rhombohedral phase of hafnia/ zirconia, which under a constrained environment exhibits wake-up-free ferroelectric behaviour. This phase could have a strong impact on the current investigations of ferroelectric binary oxide materials and pave the way toward exploiting ferroelectric behaviour for next-generation memory and logic gate applications.

Crown Copyright © 2022 Published by Elsevier Ltd.
This is an open access article under the CC BY license (http://creativecommons.org/licenses/by/4.0/)

Owing to the unexpected discovery, in 2011, of ferroelectricity at the nano-scale in Si-HfO_2 [1] there has been tremendous interest in understanding the origin of this ferroelectricity. Several dopants other than Si were studied to induce ferroelectricity in HfO_2, e.g. Al, [2] Gd, [3] Sr, [4] Y, [5] La, [6]. Perhaps of most interest is $(Hf_xZr_{1-x})O_2$ with x ranging from 0 up to 1 [7–9]. From hereon, for $(Hf_xZr_{1-x})O_2$ with $x = 0.5$, we term the composition HZO. Of course, at $x = 1$, we have pure ZrO_2, and in fact ferroelectricity has been found in pure films of ZrO_2 also [10–12] In doped HfO_2 a large remnant polarization (P_r) of 50–60 μC/cm^2 [13,14] can be achieved which is around the same level as in classic perovskite ferroeelctrics [13,14].

Fig. 1 shows the crystal structures usually observed in HfO_2 films. [13] We note that a rhombohedral polar structure (R3m) in HfO_2 has, so far, only been demonstrated theoretically. The particular phase of HfO_2 which is achieved in films depends upon various factors such as doping, surface energy and stress [14]. The ferroelectric behaviour of these materials is unusual because the stable crystallographic phase in the HfO_2 and ZrO_2 systems at room temperature and ambient pressure is a non-polar monoclinic phase (m-phase) (space group number 14, $P2_1/c$) [15]. The emergence of ferroelectricity in HfO_2 has been associated with the formation of an orthorhombic phase (o-phase) with a non-centrosymmetric space group $Pca2_1$, induced in a constrained environment [15,16]. Dopant concentration, strain, electrode materials and the upper capping layer are all reported to influence the polymorphism in doped HfO_2 films. Although the rhombohedral phase has not been observed in pure HfO_2 films, it has been observed in HZO films with a Pr of 34 μC/cm^2. The existence of this phase will be the subject of discussion later. It is noteworthy, also, that a metastable antiferroelectric phase in bulk and thin films with a tetragonal structure is also known to exist, as evidenced in Fig. 1 [17].

Recently, H. J. Lee et al. theoretically explained that the polarization is present in two-dimensional (2D) sliced regions separated by non-polar spacers. Hence, the ferroelectricity is associated with flat polar phonon bands that allow for homogeneous switching of electric dipoles [18]. In this way, dipolar order can occur without the need for co-operative 3D behaviour, allowing miniaturization and multivalued non-volatile storage [19]. In fact, the minimum thickness for ferroelectricity to occur is ~1 nm, making hafnia and zirconia-based systems highly promising for extremely down-scaled ferroelectric based devices [20,21]. We note that ferroelectricity at this low thickness level is ex-

* Corresponding authors.
E-mail addresses: josesilva@fisica.uminho.pt (J.P.B. Silva), jld35@cam.ac.uk (J.L. MacManus-Driscoll).

https://doi.org/10.1016/j.apmt.2022.101394
2352-9407/Crown Copyright © 2022 Published by Elsevier Ltd. This is an open access article under the CC BY license (http://creativecommons.org/licenses/by/4.0/)

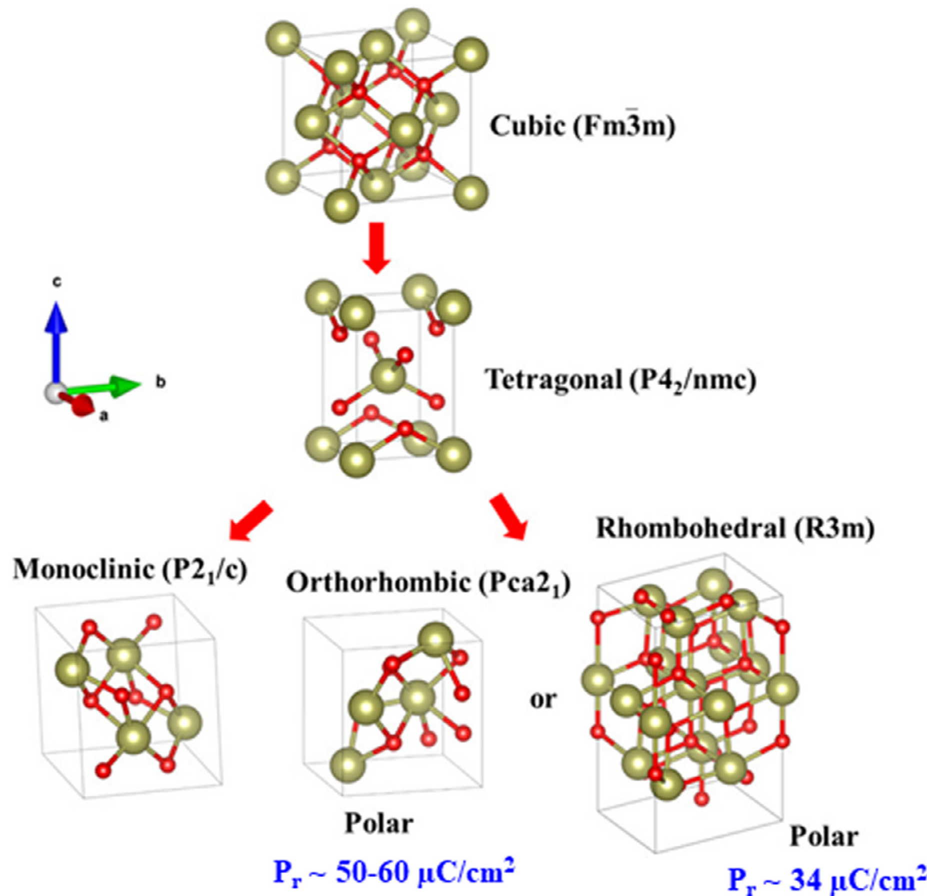

Fig. 1. Crystal structures observed in common HfO_2 films. The rhombohedral polar structure has only been theoretically demonstrated for HfO_2 and experimentally demonstrated for HZO. Reprinted (adapted) from Ref. [13] with permission from John Wiley & Sons, Inc., 2021.

tremely challenging in conventional perovskite-based ferroelectric films.

The interest in ferroelectric hafnia and zirconia-based thin films stems also from their compatibility with complementary metal oxide semiconductor (CMOS) technology, since low processing temperature, which is required for Si processing (∼400 °C), has been demonstrated [22,23]. Moreover, they have shown to be promising candidates for non-volatile random access memories, tunnel junctions and field effect transistors, and energy storage capacitors [24–27]. On the other hand, an initial wake-up pre-cycling is usually required to induce a ferroelectric behaviour in thin films of the standard orthorhombic phase of HZO [28], which is technologically problematic.

The wake-up effect is a process of opening the intially pinched hysteresis with a low P_r and this P_r is gradually increased up to saturation during cycling. This is problematic for integrating these materials into reliable memory technologies, which require stable polarization hysteresis cycles [29]. Fig. 2 shows the evolution of the polarization hysteresis loops for a TiN/Si:HfO_2/TiN structure. It is possible to observe that in the pristine state, the hysteresis loop is characterized by a clear constriction and polarity asymmetry of the coercive voltage. Under continuous cycling, P_r tends to increase until its reaches the saturation, which occurs after 10^4 cycles, where also the positive and negative coercive voltage become identical [30].

In addition, in orthorhombic HZO films the switching voltages are high. However, in more recent studies of orthorhombic HZO, wake-up free films have been demonstrated [31–41]. Furthermore, rhombohedral films have also shown to be wake-up free [42–48].

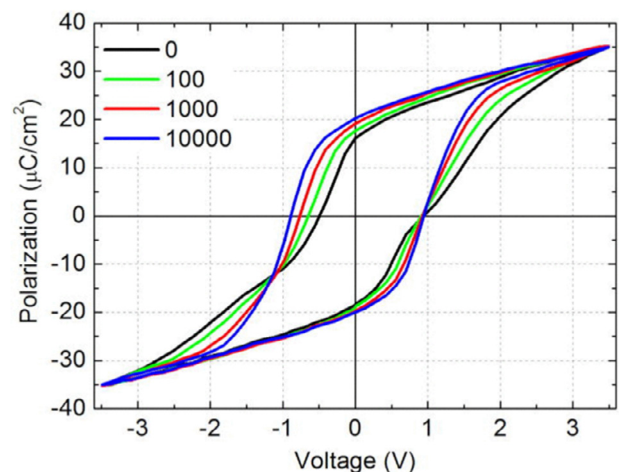

Fig. 2. Evolution of polarization-voltage (*P–V*) hysteresis for the TiN/Si:HfO_2/TiN structure with increasing number of bipolar pulse voltage cycling. The voltage amplitude and frequency of the cycling pulses were 2.5 V and 0.1 kHz, respectively. Reprinted from Ref. [30] with the permission of AIP Publishing, 2013.

giving promise for future applications. Table 1 summarizes the ferroelectric properties of wake-up free HZO and ZrO_2 films.

Recently, J. Cao et al. and I. Fina et al. revisited the recent developments on epitaxial growth of $(Hf_xZr_{1-x})O_2$ thin films [13,49]. The effect of processing parameters such as temperature and oxygen pressure on the phase stability and interface matching, as well as

Table 1.
Ferroelectric properties of exemplar wake-up free hafnia and zirconia-based thin films. P_s = spontaneous polarization; P_r = remnant polarization energy storage density; E_c = coercive field.

Device	Film thickness(nm)	P_s (μC/cm^2)	P_r (μC/cm^2)	E_c (MV/cm)	Retention (cycles)	Endurance (years)	Ref. nº
Orthorhombic thin films							
TiN/$Hf_{0.5}Zr_{0.5}O_2$/TiN	12.3	>21	>21	~1.5	5 × 10^5	–	[28]
W/$Hf_{0.5}Zr_{0.5}O_2$/W	10	~30	~22	1.0	–	–	[31]
W/$Hf_{0.5}Zr_{0.5}O_2$/W	10	32	32	~2.0	10^4	–	[32]
TiN/La-doped HfO_2-ZrO_2/TiN	10	~25	14	~0.8	10^{11}	–	[33]
TiN/$Hf_{0.5}Zr_{0.5}O_2$/TiN	12	~12	11	~1.9	10^6	-	[34]
Pt/$Hf_{0.5}Zr_{0.5}O_2$/LSMO	9	>35	20	3.0	10^8	10	[35]
Pt/$Hf_{0.5}Zr_{0.5}O_2$/LSMO	4.6	~55	13.5	~3.0	10^{11}	10	[38]
Rhombohedral thin films							
LSMO/$Hf_{0.5}Zr_{0.5}O_2$/LSMO	5	~34	34	~5.0	10^5	–	[42]
Au/ZrO_2/Nb:STO	8	~20.5	10.8	~1.5	10^6	–	[47]
Pt/ZrO_2/LSMO	14	~20	~20	~2.5	–	–	[48]

the thickness dependence of the ferroelectric properties were reviewed. However, to date less attention has been paid to the wake-up effect and underlying factors which enable wake-up free films to be achieved.

This review discusses recent developments for wake-up free ferroelectric hafnia and zirconia-based thin films. It proposes new directions for achieving wake-up free thin films without the presence of secondary phases which are often present and it presents an analysis and understanding of the formation and wake-up free nature of the rhombohedral phase in hafnia and zirconia-based thin films. Finally, it proposes a path towards achieving a CMOS compatible technology.

1. Ferroelectric *orthorhombic* hafnia and zirconia-based thin films

The need for a wake-up effect is a current disadvantage for standard orthorhombic hafnia and zirconia-based thin films. Different strategies are being investigated to reduce or eliminate the need of a wake-up cycling to achieve ferroelectric cycling. Up to now, researchers have been focusing on microstructure tailoring, defect, bulk and interface engineering, doping, NH_3 plasma treatment and epitaxial growth.

1.1. Influence of the capacitor structures on the microcrystalline structure of the films

J. Bouaziz et al. discovered that a microcrystalline effect can cause a significant reduction of the wake-up effect in HZO films [31]. In this work, non-mesa (NM) and full-mesa (M) structures were grown, as shown in Fig. 3(a) and (b), respectively. In the mesa structure (b), the M pillars are built with TiN fully covering the HZO layer, whereas the in the NM structure, the TiN only partially covers the HZO layer. Hence, different stress states are induced between a) and b) which leads to two different microcrystalline patterns.

Figs. 3(c) and (d) show the *P-E* curves for both samples obtained by the positive-up, negative-down (PUND) ferroelectric measurement methods and by the calculation method for PUND measurement (PN) that use the current response to pulse positive, P, and negative, N. It is possible to observe that the *P-E* curves obtained by the PUND method show very pinched loops for both M and NM structures with similar loops, indicative that the samples are well-saturated. In the case of the M structure, grazing incidence X-ray diffraction (GIXRD) shows no monoclinic peaks, while in the NM structure the GIXRD pattern shows many monoclinic orientations. This led to a drastic decrease in the wake-up effect, as shown in Fig. 3(e). For a number of cycles below 10^3, the M structure shows a much higher 2P_r value, which can be assigned to the absence of the monoclinic phase. However, breakdown occurs after 5 × 10^5 cycles for the M structure, while the NM structure breaks down only after 1 × 10^7 cycles. This was attributed to the fact that M structure has a higher P_r under low-stress conditions, whereas the NM structure exhibited maximum P_r under high-stress conditions. Thus, the maximum P_r seems to be more dependant on the stress conditions than on the structure configuration (M or NM).

1.2. Defects and interfacial engineering as a pathway for reducing oxygen defects in the films

A new concept to achieve wake-up free HZO films in a W/HZO/W capacitor structure was studied through defect engineering. A. Kashir et al. investigated the effect of defects, controlled by ozone dosage during the growth, on the field cycling behaviour of atomic layer deposited HZO films [32]. In this work, it is suggested that carbon contaminants and oxygen vacancies cause a large wake-up effect in the samples grown in insufficient ozone environments (exposure time below 5 s). The major reason for wake-up effect was ascribed to a structural change during electric field cycling (through either oxygen redistribution or direct electric field-driven structural transformation). By tuning the oxygen pulse length in the ALD growth during the deposition of HZO it was possible to achieve almost wake-up free ferroelectric thin films. The HZO film that was grown at 30 s ozone pulse duration shows about 98% of the woken-up P_r is in the pristine state. This behaviour was attributed to a decrease in oxygen vacancies and carbon concentration in the films. Usually, the presence of oxygen vacancies causes inhomogeneous internal fields and this inhibits the domain switching. This leads to a pinched hysteresis in the pristine material. During the electric field cycling process, the oxygen vacancies will redistribute and thus this reduces the internal field in the film. This leads to depinning of domains and contributes to the polarization [32]. Usually DC wake-up under normal temperatures is considered as a partial wake-up process and there can be further wake up with AC pulses. During the DC pulses, the oxygen ions accumulate at one electrode, which will induce the screening field and limit the generation of further oxygen vacancies. In the case of an AC wake-up, dead layers are formed beside both electrodes and the two induced screening fields will compensate [50].

In a following study, A. Kashir et al. reported on wake-up free orthorhombic HZO thin films with the highest P_r value (≈ 32 μC/cm^2) to date, which was achieved through tuning of the ozone pulse duration and the annealing temperature/time during a rapid thermal annealing (RTA) process. The significant suppression of the monoclinic and tetragonal phases in the HZO thin film after the RTA process is related to the carbon removal from the as-deposited

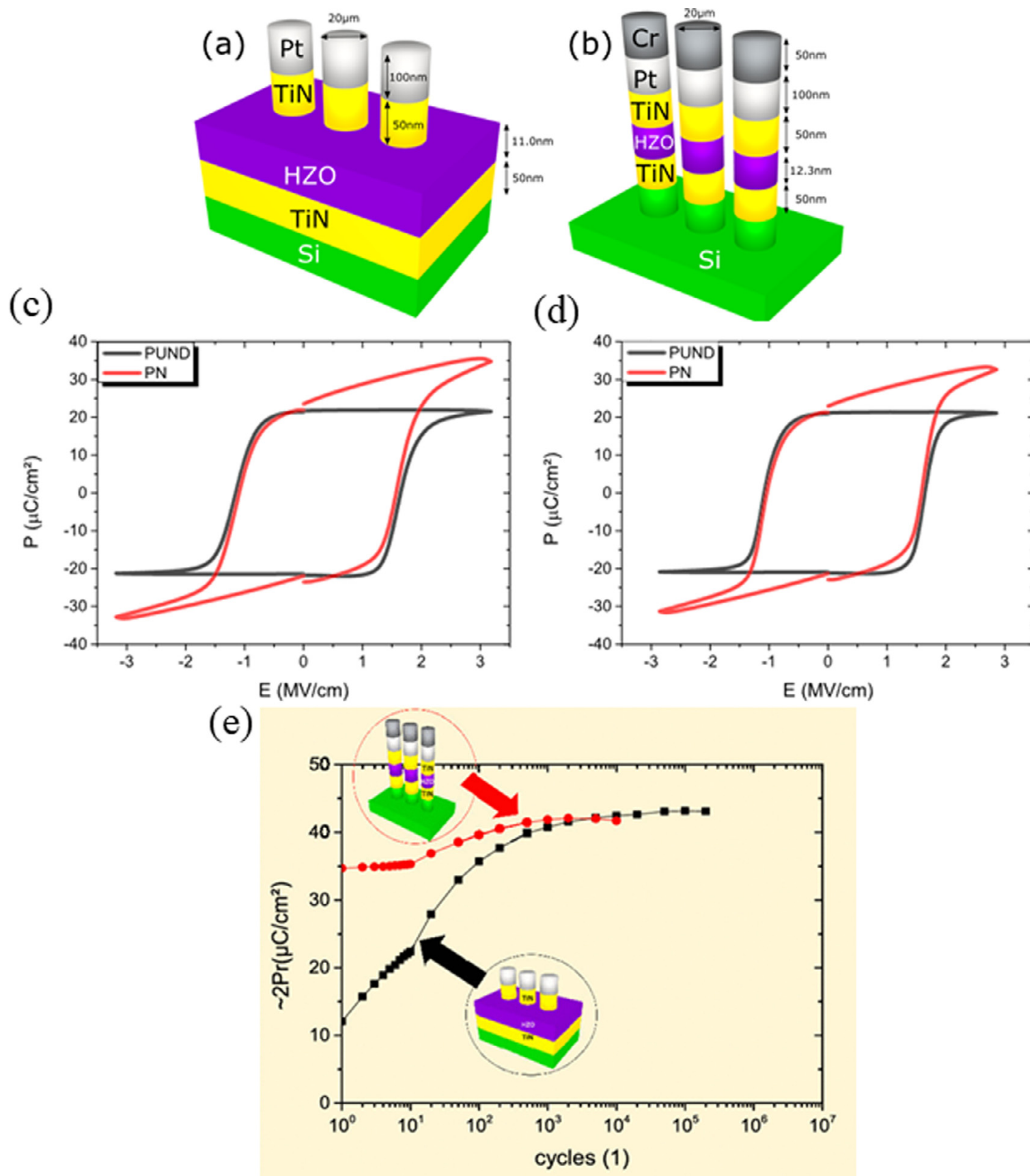

Fig. 3. Scheme of (a) non-mesa (NM) and (b) mesa (M) structures. *P-E* loops for (c) the NM structure at 10^5 cycles and (d) M structure at 2×10^3 cycles. $2P_r$ value as a function of number of cycles for non-mesa (NM) and mesa (M) structures of HZO. Reprinted (adapted) from Ref. [31] with permission from American Chemical Society, 2019.

film by increasing the ozone dosage and the in-plane tensile strain applied to the film by the tungsten (W) bottom and capping electrode [33]. In this new bulk and interface engineering approach, the authors controlled the carbon contaminants and oxygen vacancies in the films through ozone dosage and used a W capping electrode with a relatively low thermal expansion coefficient (TEC). The selection of a relatively low TEC of the capping electrode compared to the film induces an in-plane tensile strain on the film during the cooling step of thermal annealing, which appears to facilitate the formation of the orthorhombic phase by the suppression of the twinning mechanism, which is responsible for the monoclinic phase formation. It was found that by optimizing the temperature and time in a rapid thermal annealing (RTA) process, a remarkable increase in the pristine $2P_r$ value up to ~64 μC/cm^2 was achieved which compares to values of <60 μC/cm^2 for typical HZO films [51]. This is demonstrated in Fig. 4. Here, a W/HZO/W capacitor was fabricated under 15 s ozone dosage followed by RTA performed at 700 °C for 5 s. Moreover, the endurance tests revealed an almost wake-up free device until its breakdown at 10^4 cycles.

M. Yadav et al. reported on the effect of using different bottom electrodes (BE), such as metal oxide electrode (IrO_x), metal electrodes (W, Pt) and metal nitride electrode (TiN) on the ferroelectric performance of W/HZO/BE structures. W/HZO/IrO_x devices show the highest $P_r \sim 26.5$ μC/cm^2, wake-up free endurance cycling characteristics, and low leakage current with demonstration of low annealing temperature requirement as low as 350 °C. The highest value of P_r is attributed to the strong tensile strain due to the comparable thermal expansion coefficients of IrO_2 or IrO_x with W and the suppressed depolarization effect and interfacial layers

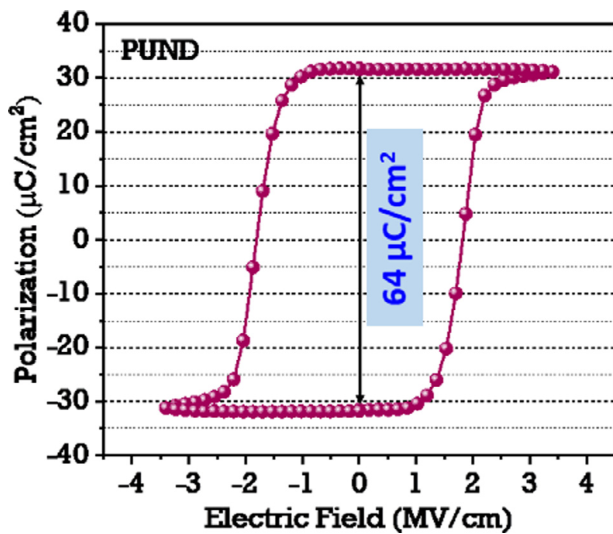

Fig. 4. *P-E* loops for the W/$Hf_{0.5}Zr_{0.5}O_2$/W structure showing high 2P_r values after a RTA at 700 °C for 5 s. Reprinted (adapted) from Ref. [33] with permission from American Chemical Society, 2021.

that can lead to the introduction of a high number of oxygen vacancies in the device stack. Moreover, IrO_x, which is a metal oxide electrode, is believed to supply oxygen to the HZO layer [52].

1.3. Doping as a strategy for improving the crystalline quality of the HZO films

Wake-up free ferroelectric orthorhombic hafnia and zirconia-based thin films can also be obtained by careful doping. M. G. Kozodaev et al. showed that La-doping can be very effective in inhibiting the unwanted monoclinic phase formation and in decreasing the leakage current in HfO_2-ZrO_2 films. [34] Moreover, the high coercive field was decreased by ~35% at the optimum La-concentration of 0.7 mol.% to an average value of ~0.7 MV/cm. As a result, a highly promising field cycling endurance up to 10^{11} cycles could be secured while maintaining a high P_r value (≥ 25 μC/cm^2).

1.4. Plasma treatment to reduce oxygen defects in the films

K.-Y. Chen et al. demonstrated that in TiN/HZO/TiN capacitors, NH_3 plasma treatment is a successful approach to significantly reduce the oxygen vacancies in HZO films. [35] At the top and bottom interfaces in TiN/HZO/TiN are asymmetrical owing to the different processing steps which render the top of the HZO film more oxygen deficient than the bottom. Overall, the NH_3 plasma treatment eliminates the wake-up effect by reducing oxygen vacancy formation in HZO films with TiN electrodes. At first, TiN is reactive to oxygen and forms TiO_xN_y at both TiN/HZO interfaces, causing oxygen deficient HZO, but this is more pronounced at the bottom interface because the bottom interface experiences *both* thermal ALD and post-metallization annealing whereas the top interface experiences only the post-metallization one. However, the interfacial treatment of the bottom interface with NH_3 plasma suppresses the formation of TiO_xN_y at that interface, and this suppresses the formation of oxygen deficient HZO. At the top interface, the HZO partially reacts with TiN to form $HfZrO_xN_y$. This helps inhibit interfacial reaction of HZO with the top TiN, again the amount of oxygen vacancies in the upper part of the HZO film. Overall, the more oxygen stoichometric films are both wake-up and fatigue free. A further effect of the NH_3 plasma treatment is that it reduces the fatigue effect because it suppresses the pinning of domain walls by oxygen vacancies. Overall, a wake-up free 2P_r of 20.2 μC/cm^2 was achieved by NH_3 plasma treatment at both top and bottom interfaces, with no fatigue effect up to 10^6 cycles. This value is lower than the 2P_r values of ~64 μC/cm^2 discussed above, likely because this process is insufficient to eliminate all the oxygen vacancies in the films. In addition, in this work it was not clear if phases such as the monoclinic phase are present which would significantly reduce the 2P_r value.

1.5. Epitaxial growth as a route to achieve phase pure films

Recently, J. Lyu et al. investigated the ferroelectric properties of orthorhombic epitaxial HZO films grown on $La_{0.7}Sr_{0.3}MnO_3$/$SrTiO_3$ (LSMO/STO) [36–38]. A maximum *Pr* of 20 μC/cm^2 was achieved without the need of a wake-up process. The polarization window (difference between positive and negative polarization) extrapolated to 10 years was around 41% (2*Pr*> 15 μC/cm^2) of the initial window, while after 10^8 cycles the polarization window decreased up to 36% of the initial value due to ferroelectric fatigue [36].

The different behaviors between polycrystalline and epitaxial films could be due to either the different microstructures (epitaxial or polycrystalline films), or the different electrodes typically used for these different film forms, or both these effects. LSMO or TiN bottom electrodes are commonly used for epitaxial films or polycrystalline films, respectively. While, as discussed above, TiN electrodes can induce the formation of oxygen vacancies in HZO in proximity to it, LSMO is not expected to do so [39].

In another epitaxial film study, the growth window (deposition temperature and oxygen pressure) of epitaxial stabilization of HZO films on LSMO/STO(001) substrates was investigated. The deposition parameters, such as oxygen pressure, substrate temperature and also thickness were found to have great impact on the amount of the orthorhombic phase present. The *Pr* increased with the amount of orthorhombic phase and was found to increase up to ~24 μC/cm^2 [37]. The authors also investigated the retention and fatigue in the growth window of HZO epitaxial films and concluded that a film with 9 nm thickness does not show a significant wake-up effect but exhibits pronounced fatigue that increases markedly with substrate temperature and pressure, while the retention degrades in films deposited at low pressure.

Fig. 5 (a) and (b) illustrate the evolution of ferroelectric behaviour in HZO films on LSMO/STO(001). The normalized *Pr* in the pristine state (black squares, left axis), *Pr* after 10^7 cycles (blue triangles, right axis), and normalized *Pr* after 10 years of positive (red solid circles, right axis) and negative (red empty circles, right axis) poling as a function of oxygen pressure and substrate temperature, respectively, are shown. The defects located at grain boundaries are proposed to be critical to ferroelectric behaviour, causing pinning of ferroelectric domains which reduces fatigue. Moreover, it seems also that optimal conditions to reduce fatigue produce, in the pristine state. lower *Pr* values [38].

Integration of wake-up free epitaxial HZO films on Si has also been attempted [39,40]. HZO/LSMO was grown on YSZ-buffered Si(001) and HZO/LSMO/$LaNiO_3$ on YSZ-buffered Si(001). CeO_2 and $LaNiO_3$ layers were introduced to progressively reduce the lattice mismatch between LSMO and YSZ, making possible epitaxial growth of LSMO with a [001] orientation. However, a minority monoclinic phase was present in the predominantly orthorhombic, 9.5 nm thick HZO films. The films exhibited a *Pr* of 20 μC/cm^2, with an extrapolated 2*Pr* of around 14 μC/cm^2 after 10 years. However, the 2P_r is equal to 2 μC/cm^2 after 10^9 cycles. [40] Recently, it was discovered that by reducing the thickness of the HZO film to 4–8 nm on HZO/LSMO/$LaNiO_3$/YSZ-buffered Si(001), in the pristine state, the following ferroelectric parameters were achieved: a 2*Pr* of 27 μC/cm^2, an endurance of 2Pr > 6 μC cm^{-2} after 10^{11} cycles, and a retention of 2*Pr* > 12 μC/cm^2 extrapolated to 10 years [39].

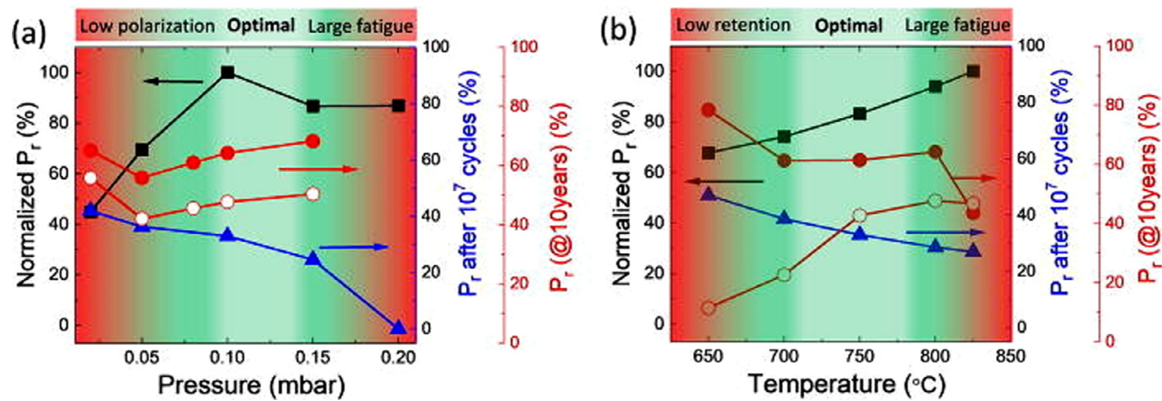

Fig. 5. Dependences of the normalized *Pr* in the pristine state (black squares, left axis) and *Pr* after 10^7 cycles (blue triangles, right axis), and normalized *Pr* after 10 years of positive (red solid circles, right axis) and negative (red empty circles, right axis) poling as a function of (a) oxygen pressure and (b) substrate temperature for HZO films on LSMO/STO(001). Coloured areas summarize the main effect of the deposition parameters on polarization, fatigue, and endurance. Reprinted from Ref. [38] with the permission of AIP Publishing, 2017.

1.6. Doping and epitaxial growth as a combined strategy to achieve high-performance phase pure films

As demonstrated above, La-doping is a useful strategy to achieve wake-up free ferroelectric films. T. Song et al. applied the epitaxial growth strategy to La-doped HZO films. They showed that 8.3 nm thick La-doped HZO films do not show a wake-up effect, accompanied by good endurance (>10^{10} cycles) and retention (>10 years) [41].

As discussed previously, the orthorhombic phase is usually required to induce ferroelectricity, while the monoclinic one is assumed to be a parasitic phase. According to Fengler et al. the cause of the wake-up effect is crystallographic phase change contributions and/or the presence of oxygen vacancies [53]. Overall, most of the research on wake-up free orthorhombic hafnia and zirconia-based films has focused on eliminating both the monoclinic phase and oxygen vacancies through microstructure and composition control, doping, interfacial engineering, NH_3 plasma treatment and epitaxial growth control. However, more detailed studies about the suppression of the wake-up effect in hafnia and zirconia-based films are still needed. Hence, defect engineering of films via a variety of means, e.g. ion bombardment, doping additives or via careful process control, in particular the effect of substrate temperature during post-annealing, as well as the use of different buffer layers could give insight into the mechanisms of the wake-up process.

So far, we have focused on the ferroelectric properties of *orthorhombic* HZO films and the possible different effects, which give rise to a wake-up free robust ferroelectric polarization. Now we explore reports of *rhombohedral* structured hafnia and zirconia-based films which show wake-up free ferroelectric behaviour.

2. The *rhombohedral* phase of hafnia and zirconia-based thin films

2.1. Influence of substrate strain on the stabilization of the HZO phase

In 2018, Y. Wei and co-workers [42] discovered a new polar rhombohedral (R3 or R3m) phase in epitaxially-strained HZO thin films deposited on (001)-oriented $La_{0.7}Sr_{0.3}MnO_3/SrTiO_3$ (LSMO/STO) substrates deposited by pulsed laser deposition (PLD). At the initial stages of the growth, after the formation of a fully coherent, atomically thin interfacial layer, an undistorted cubic phase forms, but as the film thickens the growing crystallites are subjected to a large epitaxial compressive strain that elongates the cubic unit cell along the out-of-plane[111] direction, inducing rhombohedral symmetry with a polar unit cell.

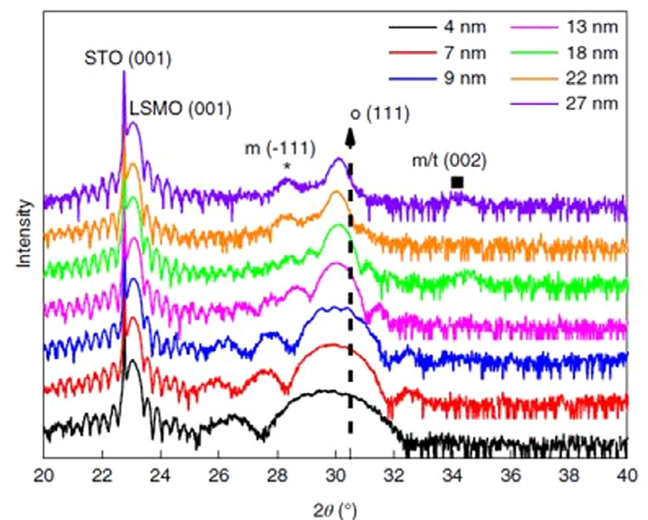

Fig. 6. XRD patterns of the $Hf_{0.5}Zr_{0.5}O_2$ films deposited on $La_{0.7}Sr_{0.3}MnO_3/SrTiO_3$ substrates. Reprinted from Ref. [42] with permission from Springer Nature Limited, 2018.

Fig. 6 depicts the XRD patterns of HZO films with thicknesses ranging from 4 nm to 27 nm. It is possible to observe that as the thickness decreases, the HZO (111) peaks shift to smaller angles, which indicates a higher compressive in-plane strain for the thinnest layers. Due to the favourable epitaxial relationships induced by the STO/LSMO stack, the growing crystallites are subjected to a large epitaxial compressive strain at low thickess that elongates the cubic unit cell along the out-of-plane[111] direction, inducing rhombohedral symmetry with a polar unit cell [42]. As the thickness increases the effect of the substrate decreases. For films thicker than 9 nm, new peaks from the monoclinic phase appear.

Given the proximity of the HZO peak to the position of the expected peak for the o-phase, pole figure measurements and synchrotron XRD measurements were done in order to understand the phase evolution. It was possible to conclude that the HZO film has a rhombohedral phase. Further, cross-sectional high-angle annular dark-field scanning TEM (HAADF-STEM) together with fast Fourier transform (FFT) analyses shown in Fig. 7(a) revealed that d_{111} = 2.95–3.01 Å and d_{11-1} = 2.92–2.96 Å, which confirm the

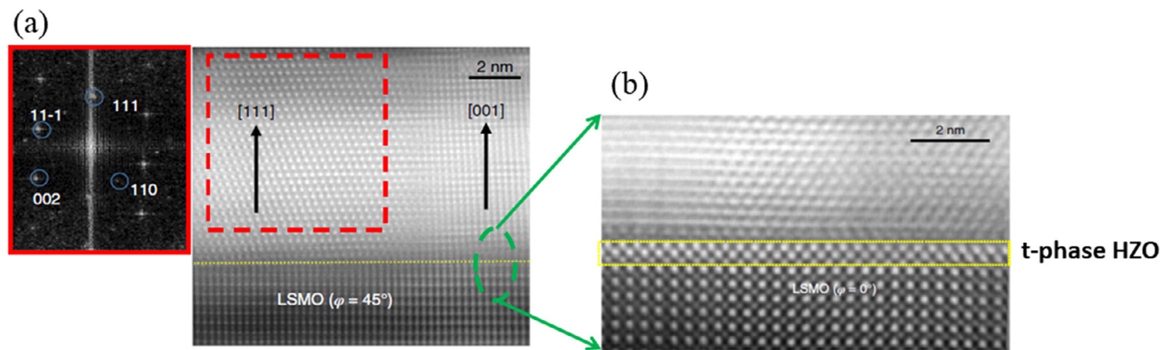

Fig. 7. (a) Cross-sectional HAADF-STEM image of 9-nm-thick $Hf_{0.5}Zr_{0.5}O_2$ film, observed along the [110] zone of the substrate ($\varphi = 45°$). Inset (left): Fourier transform of the [111] domain. (b) Cross-HAADF-STEM image observed along STO [100], revealing a clear interfacial t-phase of HZO. Reprinted (adapted) from Ref. [42] with permission from Springer Nature Limited, 2018.

non-orthorhombic nature of this phase, and corroborates the synchrotron XRD analysis.

Standard first-principles methods considering two rhombohedral structures (R3m and R3) confirmed the rhombohedral phase. The substitution of Hf by Zr results in the R3 phase and favors the formation of the weakly polar R3m phase. The R3m phase of bulk-like HZO is characterized by $d_{111} \approx 2.94$ Å and $P \approx 1$ μ Ccm^{-2}. To understand the effect of epitaxial compression, simulations for a number of fixed values of the lattice constants in the (111) plane of the HZO structure were undertaken. The calculations show that when d_{111} increases to a value of ≈ 3.25 Å, a clear structural transition occurs to a phase that retains the R3m symmetry but is strongly polar, with $P \approx 15$ μ Ccm^{-2}. We note that a d_{111} value of $\approx$ 3.25 Å is close to that in the thinnest, rhombohedral (1.5 nm) films and thus the calculations confirm the expt. result that a rhombohedral phase exists for a very high d_{111} value.

The interface between the LSMO layer and the HZO film was also evaluated by HAADF-STEM. As depicted in Fig. 7(b), a clear interfacial tetragonal (t)-phase of HZO was observed. Hence, the tensile-strained LSMO layer grown on STO leads to the formation of 2–3 monolayers of a tetragonal HZO layer. This interfacial HZO phase is completely strained to the substrate corresponding to a huge (~8%) in-plane tensile-strained tetragonal phase. This transitional tetragonal phase stabilizes a (111) orientation of the rhombohedral phase above it.

GaN, sapphire, or cubic Si (111) substrate are also effective templates for stabilizing rhombohedral HZO(111), while imposing an in-plane compressive strain [45].

2.2. The role of oxygen on the phase stabilization in HZO

The temperature-dependent phase transitions in HZO/LSMO heterostructures have been investigated by heating in vacuum *in-situ* in the TEM and complementarily in air using *in-situ* XRD [43]. Under vacuum, the LSMO layer deoxygenates even at temperatures as low as 150 ºC, resulting in a sequence of topotactic phase transformations. On the other hand, rhombohedral HZO is robust until 300 ºC, after which it exhibits oxygen vacancy ordered HZO phases, formed by loss of oxygen from HZO, with reduced rhombohedral distortions. In addition, it was revealed that there is no clear (reversible) ferro to paraelectric phase transition temperature (T_c) in rhombohedral HZO. Also, epitaxial rhombohedral HZO films grown on various substrates, such as GaN, sapphire, Si, LaAlO3, DyScO3, (LaAlO3)0.3(Sr2AlTaO6)0.7 and YAlO3 have been explored to identify global trends for stabilizing the rhombohedral phase polymorphs [44–46]. However, for some substrates and growth conditions a non-pure rhombohedral phase was achieved. The presence of other structural phases resulted in poorer ferroelectric performance.

Atomic resolution electron microscopy with in-situ electrical biasing of a LSMO/HZO/LSMO/STO capacitor structure has enabled the role of oxygen vacancies in rhombohedral phase on ferroelectric properties to be determined [54], by direct oxygen imaging upon undertaking oxygen voltammetry, reversible oxygen vacancy migration from the bottom to the top electrode through HZO led to reversible structural phase transitions in both the epitaxial LSMO and HZO layers. Hence, a positive bias of +3 V causes injection of oxygen from the bottom LSMO layer in the HZO layer and thus transforms it into from the rhombohedral phase to the more oxygen stoichiometric monoclinic/orthorhombic phases. A negative bias of −3 V restored the rhombohedral phase by removing oxygen vacancies (by reverse migration).

Further investigation on stabilizing the rhombohedral HZO phase, M. Zheng et al. shows that 35-nm-thick rhombohedral HZO films have also been stabilized on ZnO (0001) substrates, under oxygen-deficient conditions [55]. It was proposed that a strong symmetry constraint was imposed on the HZO layer during the initial epitaxial growth stage, i.e., the plane in the HZO adjacent to ZnO(0001) should have threefold symmetry. First principles calculations revealed that monoclinic and rhombohedral phases are energetically comparable with each other when this three-fold symmetry constraint is considered. Also, the first principles calculations showed that incorporation of doubly charged oxygen vacancies shifts the energy balance between monoclinic and rhombohedral competing phases, making the metastable rhombohedral phase more stable under oxygen-deficient conditions.

2.3. Influence of the substrate on the phase formation in zirconia

Density functional theory (DFT) calculations show that pure ZrO_2 are expected to be most stable as the (111)-oriented rhombohedral R3m phase [48]. The calculations also predicted that the stability window of rhombohedral ZrO_2 is up to a thickness of 32 nm, while it is less than 4 nm in pure HfO_2 and about 12 nm in the case of HZO [48]. Therefore, it is predicted that rhombohedral polar phase in ZrO_2-based thin films is stable to significantly higher thickness than Hf-rich HZO, without additional non-polar phases such as monoclinic and tetragonal ones.

In terms of the experimental validation of the theoretical calculations, in fact, there have been two reports on rhombohedral zirconia thin films. In this section we discuss the structural aspects of rhombohedral films and in the next section we discuss the ferroelectric properties.

In one study, a pure ZrO_2 film of 8-nm thickness deposited by ion-beam sputtering (IBS) on an Nb:STO (111) substrate was found to be the rhombohedral phase. Since the film was directly deposited on the substrate, a large lattice and structural mismatch resulted, and the formation of a tetragonal phase was not observed

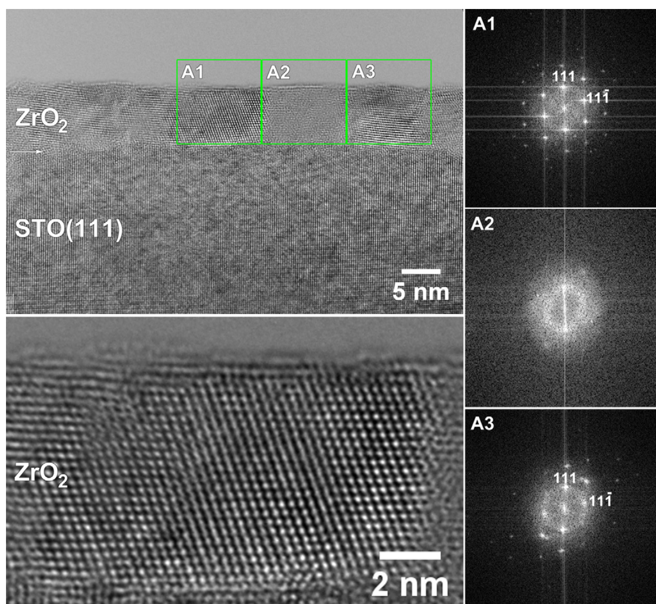

Fig. 8. HRTEM images of ZrO_2 thin film deposited on a STO (111) substrate showing crystalline areas of rhombohedral phase (e.g. A1 and A3) with mixed orientation, plus amorphous regions (e.g. A2). In the right side, the FFT patterns corresponding to the areas indicated in the HRTEM image show the crystalline rhombohedral nature of the regions A1 and A3 and the amorphous nature of region (A2). Reprinted from Ref. [47] with permission from American Chemical Society, 2021.

[47]. Instead amorphous ZrO_2 regions intercalated with the crystalline rhombohedral ones were observed, as shown in Fig. 8. Thus, the combination of the IBS technique with rapid-thermal annealing allows the growth of the rhombohedral R3m ZrO_2 phase at lower temperatures.

Similarly, to what was proposed for the growth of the rhombohedral HZO phase [42], a combination of the large surface energy induced internal pressure of the nanoparticles and the substrate imposed compressive strain are responsible for the stabilization of the rhombohdral phase in the ZrO_2 films [47].

Recently, phase pure rhombohedral ZrO_2 films can also be grown on $La_{2/3}Sr_{1/3}MnO_3$-buffered $DyScO_3$(110) substrates. The $DyScO_3$(110) substrates provides a slightly higher tensile strain compared to STO (001), which stabilizes the rhombohedral ZrO_2 phase up to a thickness of 37 nm [48].

2.4. Ferroelectric properties of hafnia and zirconia-based thin films

Fig. 9 shows polarization-electric field (*P-E*) hysteresis loops for 5 nm HZO /$La_{0.7}Sr_{0.3}MnO_3$/$SrTiO_3$ (001), and 8-nm thick ZrO_2/Nb:$SrTiO_3$(111) films. Both sets of films are ferroelectric [42,47]. Maximum P_r values of 34 and 10.8 μC/cm^2, were observed for the HZO and ZrO_2 films, respectively. Even higher P_r values of 11 and 20.75 μC/cm^2 were obtained for 37 nm and 14 nm thick ZrO_2 films grown on $La_{2/3}Sr_{1/3}MnO_3$/ $DyScO_3$(110) substrates. The moderately higher values compared the 8 nm films above is likely owing to the higher film thickness and also different strain level, since $DyScO_3$ substrate provides a slightly higher tensile strain for tetragonal phase compared to STO substrate. The increase of the tensile strain applied on LSMO bottom electrode causes the amount of non-ferroelectric phase (t-phase) decreases. It is noted that while the P_r values for HZO and ZrO_2 films are lower than perovskite films such as (Pb,Zr)TiO_3 (PZT) (P_r of $<\sim$40 μC/cm^2) and $BiFeO_3$ (BFO) ($P_r \sim$ 100 μC/cm^2), PZT contains toxic Pb, and BFO has a low bandgap and associated large leakage, which is limiting for widespread memory use [56]. Therefore, rhombohedral hafnia and zirconia-based thin films are important competitors to conventional perovskite-based ferroelectric materials.

For both HZO and ZrO_2, for the rhombohedral structure, ferroelectric behaviour emerges without the need for applying any wake-up cycling. This is different to the case of the orthorhombic structure which requires wake up cycling. This is possibly because the monoclinic phase is absent or very rarely found in the rhombohedral films [40]. In addition, no wake-up effect is required since the ferroelectric polarization is stabilized by compressive epitaxial strain. However, the role of the oxygen vacancies on the ferroelectric polarization of rhombohedral films needs to be investigated in more detail, as was done for orthorhombic films [57–60].

Positively for ZrO_2, the coercive field (E_c) is ~1.5 MV/cm which is lower than HZO's which is ~ 5 MV/cm. A lower E_c is advantageous for memory applications where low switching voltages are desired.

A current challenge for ZrO_2 films is that after 10^3 cycles the P_r value decreases by around 19% after 10^6 cycles. [47] The origin of this degradation may be similar to that observed in Au/HZO/LSMO [54] where a partial phase transition from rhombohedral to monoclininc occurs because the HZO layer itself is forced to act as source/sink of oxygen vacancies when Au is used as a top electrode, resulting in a reversible phase transition even with low voltage pulses and modest cycling. In the case of LSMO/HZO/LSMO the device becomes leaky at 10^5 cycles and further optimization of the device endurance performance through domain/interfacial engineering is proposed [42].

2.5. DFT simulations in hafnia and zirconia-based thin films

First-principles simulations were used to determine the structural phases of the crystalline ZrO_2 and HZO layers. They were also carried out to understand the polarization behaviour as a function of the d_{111} inter-plane spacing in ZrO_2, HfO_2 and HZO films [42,47,61]. From Fig. 10, it is possible to observe that larger d_{111} values correspond to a stronger out-of-plane polarization due to an in-plane epitaxial compression in ZrO_2, HfO_2 and HZO layers. Moreover, it is possible to observe that for a moderate in-plane compressive strain ($d_{111}<$ 3.1 Å) the HZO exhibits the highest P_s, while for highly compressive strain ($d_{111}>$ 3.1 Å) the HZO exhibits lower P_s values. In addition, highly compressively strained HfO_2 exhibits the highest P_s values but there are still no reports on the rhombohedral structure and its ferroelectric properties. This theoretical result suggests that the P_s evolution in the rhombohedral systems are different from the one experimentally observed in the orthorhombic phase films.

3. Challenges and perspectives for wake-up free hafnia and zirconia-based thin films

Here we propose future studies to further understand the wake-up effect in hafnia and zirconia-based films. Growth of phase-pure materials without any secondary phases or amorphous regions is crucial both for reliable performance for applications. Growth of epitaxial films by physical vapour deposition (PVD) or chemical vapour deposition (CVD) should be used in order to separately understand the factors which may influence wake-up, as outlined below. PVD is preferred for achieving the highest quality films. Finally, matching structural data, and polar properties is necessary, combined with first-principles simulations to predict structure and match this to experiment.

- The key factors to understand in relation to the wake-up effect of orthoromic and rhombohedral hafnia and zirconia-based thin films are:
  - the role of intrinsic compositional effects. Here, a range of Zr/Hf ratios should be investigated in $(Hf_xZr_{1-x})O_2$.

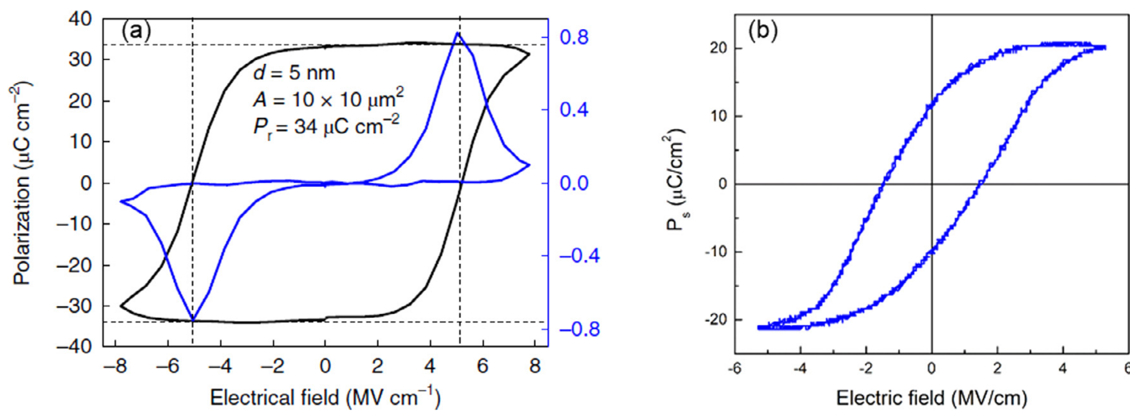

Fig. 9. *P-E* loops for (a) LSMO/HZO/LSMO/STO and (b) Au/ZrO_2/Nb:STO film capacitors. Figure (a) reprinted (adapted) from Ref. 40 with permission from Springer Nature Limited, 2018. Figure (b) reprinted (adapted) from Ref. 45 with permission from American Chemical Society, 2021.

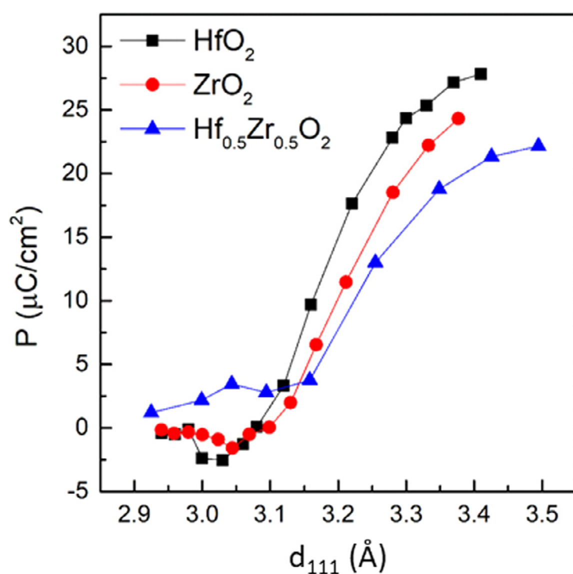

Fig. 10. Computed evolution of the out-of-plane polarization of R3m-structured ZrO_2, HfO_2 and $Hf_{0.5}Zr_{0.5}O_2$ as a function of the d_{111} inter-layer spacing, where larger d_{111} values correspond to a more compressive in-plane epitaxial strain. Reprinted (adapted) from Refs. [42,47] and [61] with permissions from Springer Nature Limited, 2018, from American Chemical Society, 2021 and from American Physical Society, 2020, respectively.

- the roles of strain and orientation engineering on *as-grown* material. Here, growth of single phase epitaxial films of orthorhombic and rhombohedral phases should explored using:
  a) different lattice and/or structurally (mis-)matched single crystal substrates and appropriate buffers. Efforts should be made to minimize second-phase inclusions.
  b) different isovalent and aliovalent chemical dopants on both the cation and anion sites.
- the role of *post-growth* strain, films with different capping layers on the film surfaces should be explored.

Finally, other challenges of $(Hf_xZr_{1-x})O_2$ and ZrO_2 relate to understanding and improving several ferroelectric parameters, e.g. endurance, phase purity, retention, coercive field and switching dynamics. To achieve this understanding, the following areas should be explored:

- *rhombohedral* films should be studied further from a theoretical point-of-view, e.g. it is important to understand if the 2D slice model detailed earlier applies also to the rhombohedral phase.
- the role of oxygen vacancies on the stabilization of the rhombohedral phase. In particular, it is known for orthorhombic films that structural transitions induced by charged oxygen vacancies can occur [62], which can degrade the performance of the device.
- the contribution of oxygen vacancies to the ferroelectric polarization of rhombohedral films need to be investigated, since it was shown that they can contribute to the polarization in orthorombic films [57,58].
- investigate the possibility of obtaining rhombohedral films on substrates other than perovskite oxides ones, such as Si, and the role of different top and bottom electrodes.
- where it is possible to reduce the processing temperature of the rhombohedral phase to be similar to orthorhombic films (i.e. ~400 ºC).
- improving the endurance and retention of films of orthorhombic wake-up free films, via undertaking precise growth control of epitaxial single-phase orthorhombic films with reduced oxygen vacancy concentrations. Also, translation of such studies to rhombohedral films.
- new strategies to reduce the magnitude of the switching voltages. Here, precise growth control to avoid secondary phases and defect formation is needed.
- similar to what have been investigated in wake-up cycled orthorhombic films [63], polarization switching kinetics should be understood in wake-up free orthorhombic and rhombohedral films.

In conclusion, discovery of wake-up free orthorhombic hafnia and zirconia-based thin films, as well as discovery of the rhombohedral phase in hafnia and zirconia-based thin films are highly significant for realizing important applications of these simple and (pseudo-)binary oxides. From both a theoretical and experimental point-of-view, there is still some way to go towards a global understanding of the growth mechanisms and ferroelectric behaviour, including how to reliably achieve wake-up-free films of both rhombohdral and orthorhombic structures, as well as the parameters that produce stable and high performance rhombohedral films. Finally, we also believe that it is possible to expand the possibility of applications of the wake-up-free films of both rhombohedral and orthorhombic structures to energy storage capacitors [64], neuromorphic devices [65] and piezoelectric devices, such as in nano-electro-mechanical-systems (NEMS) transducers, where the existence of a negative piezoelectric coefficient that can be controlled by epitaxial strain seems to be very promising [66].

Declaration of Competing Interest

The authors declare that they have no known competing financial interests or personal relationships that could have appeared to influence the work reported in this paper.

CRediT authorship contribution statement

J.P.B. Silva: Conceptualization, Investigation, Writing – original draft, Writing – review & editing. **K.C. Sekhar:** Investigation, Writing – review & editing. **R.F. Negrea:** Writing – review & editing. **J.L. MacManus-Driscoll:** Conceptualization, Writing – review & editing, Supervision. **L. Pintilie:** Writing – review & editing, Supervision.

Acknowledgements

This work was supported by the Portuguese Foundation for Science and Technology (FCT) in the framework of the Strategic Funding Contract UIDB/04650/2020 and by DST-SERB, Govt. of India through Grant Nr. ECR/2017/00006. R. F. Negrea and L. Pintilie acknowledge funding through project CEPROFER/ PN-III-P4-ID-PCCF-2016-0047 (contract 16/2018, funded by UEFISCDI). J.L.M-D. thanks the Royal Academy of Engineering Chair in Emerging Technologies Grant, CIET1819_24, the EPSRC grant EP/T012218/1- ECCS – EPSRC, and the grant EU-H2020-ERC-ADG # 882929, EROS.

References

[1] T.S. Boescke, J. Mueller, D. Braeuhaus, U. Schroeder, U. Boettger, Ferroelectricity in hafnium oxide thin films, Appl. Phys. Lett. 99 (2011) 102903.
[2] S. Mueller, C. Adelmann, A. Singh, S. Van Elshocht, U. Schroeder, T. Mikolajick, Ferroelectricity in Gd-doped HfO_2 thin films, ECS J. Solid State Sci. Technol. 1 (2012) N123.
[3] S. Mueller, J. Mueller, A. Singh, S. Riedel, J. Sundqvist, U. Schroeder, T. Mikolajick, Incipient Ferroelectricity in Al-Doped HfO_2 thin films, Adv. Funct. Mater. 22 (2012) 2412.
[4] T. Schenk, S. Mueller, U. Schroeder, R. Materlik, A. Kersch, M. Popovici, C. Adelmann, S. Van Elshocht, T. Mikolajick, Strontium doped hafnium oxide thin films: wide process window for ferroelectric memories, in: European Solid-State Device Research Conference, 2013, p. 260.
[5] T. Shimizu, K. Katayama, T. Kiguchi, A. Akama, T.J. Konno, O. Sakata, H. Funakubo, The demonstration of significant ferroelectricity in epitaxial Y-doped HfO_2 film, Sci. Rep. 6 (2016) 32931.
[6] J. Muller, T. Boscke, S. Muller, E. Yurchuk, P. Polakowski, J. Paul, D. Martin, T. Schenk, K. Khullar, A. Kersch, W. Weinreich, S. Riedel, K. Seidel, A. Kumar, T. Arruda, S. Kalinin, T. Schlosser, R. Boschke, R. van Bentum, U. Schroder, T. Mikolajick, Ferroelectric hafnium oxide: a CMOS-compatible and highly scalable approach to future ferroelectric memories, in: 2013 IEEE International Electron Devices Meeting (IEDM), 2013, p. 10.8.1.
[7] Q. Luo, H. Ma, H. Su, K.-H. Xue, R. Cao, Z. Gao, J. Yu, T. Gong, X. Xu, J. Yin, P. Yuan, L. Tai, D. Dong, S. Long, Q. Liu, X.-S. Miao, H. Lv, M. Liu, Composition-dependent ferroelectric properties in sputtered $Hf_XZr_{1-X}O_2$ thin films, IEEE Electron Device Lett. 40 (2019) 570–573.
[8] J. Müller, T.S. Böscke, U. Schröder, S. Mueller, D. Bräuhaus, U. Böttger, L. Frey, T. Mikolajick, Ferroelectricity in simple binary ZrO_2 and HfO_2, Nano Lett. 12 (2012) 4318–4323.
[9] J. Bouaziz, P.R. Romeo, N. Baboux, R. Negrea, L. Pintilie, B. Vilquin, Dramatic impact of pressure and annealing temperature on the properties of sputtered ferroelectric HZO layers, APL Materials 7 (2019) 081109.
[10] S. Starschich, T. Schenk, U. Schroeder, U. Boettger, Ferroelectric and piezoelectric properties of $Hf_{1-x}Zr_xO_2$ and pure ZrO_2 films, Appl. Phys. Lett. 110 (2017) 182905.
[11] J.P.B. Silva, J.M.B. Silva, K.C. Sekhar, H. Palneedi, M.C. Istrate, R.F. Negrea, C. Ghica, A. Chahboun, M. Pereira, M.J.M. Gomes, Energy storage performance of ferroelectric ZrO_2 film capacitors: effect of HfO_2:Al_2O_3 dielectric insert layer, J. Mater. Chem. A 8 (2020) 14171–14177.
[12] M. Hoffmann, F.P.G. Fengler, M. Herzig, T. Mittmann, B. Max, U. Schroeder, R. Negrea, L. Pintilie, S. Slesazeck, T. Mikolajick, Unveiling the double-well energy landscape in a ferroelectric layer, Nature 565 (2019) 464–467.
[13] J. Cao, S. Shi, Y. Zhu, J. Chen, An overview of ferroelectric hafnia and epitaxial growth, Phys. Status Solidi RRL (2021) 2100025.
[14] M.H. Park, T. Schenk, C.M. Fancher, E.D. Grimley, C. Zhou, C. Richter, J.M. LeBeau, J.L. Jones, T. Mikolajick, U. Schroeder, A comprehensive study on the structural evolution of HfO_2 thin films doped with various dopants, J. Mater. Chem. C 5 (2017) 4677–4690.
[15] S. Estandía, N. Dix, M.F. Chisholm, I. Fina, Florencio Sánchez, Domain-matching epitaxy of ferroelectric $Hf_{0.5}Zr_{0.5}O_2$(111) on $La_{2/3}Sr_{1/3}MnO_3$(001), Cryst. Growth Des. 20 (2020) 3801–3806.
[16] M.H. Park, H.J. Kim, G. Lee, J. Park, Y.H. Lee, Y.J. Kim, T. Moon, K.D. Kim, S.D. Hyun, H.W. Park, H.J. Chang, J.-H. Choi, C.S. Hwang, A comprehensive study on the mechanism of ferroelectric phase formation in hafnia-zirconia nanolaminates and superlattices, Appl. Phys. Rev. 6 (2019) 041403.
[17] K. Chae, J. Hwang, E. Chagarov, A. Kummel, K. Cho, Stability of ferroelectric and antiferroelectric hafnium–zirconium oxide thin films, J. Appl. Phys. 128 (2020) 054101.
[18] H.-J. Lee, M. Lee, K. Lee, J. Jo, H. Yang, Y. Kim, S.C. Chae, U. Waghmare, J.H. Lee, Scale-free ferroelectricity induced by flat phonon bands in HfO_2, Science 369 (2020) 1343–1347.
[19] B. Noheda, J. Íñiguez, A key piece of the ferroelectric hafnia puzzle, Science 369 (2020) 1300–1301.
[20] S.S. Cheema, D. Kwon, N. Shanker, R. Reis, S.-L. Hsu, J. Xiao, H. Zhang, R. Wagner, A. Datar, M.R. McCarter, C.R. Serrao, A.K. Yadav, G. Karbasian, C.-H. Hsu, A.J. Tan, L.-C. Wang, V. Thakare, X. Zhang, A. Mehta, E. Karapetrova, R.V. Chopdekar, P. Shafer, E. Arenholz, C. Hu, R. Proksch, R. Ramesh, J. Ciston, S. Salahuddin, Enhanced ferroelectricity in ultrathin films grown directly on silicon, Nature 580 (2020) 478–482.
[21] S.S. Cheema, N. Shanker, C.-H. Hsu, A. Datar, J. Bae, D. Kwon, S. Salahuddin, One nanometer HfO_2-based ferroelectric tunnel junctions on silicon, Adv. Electron. Mater. (2021) 2100499.
[22] T. Onaya, T. Nabatame, N. Sawamoto, A. Ohi, N. Ikeda, T. Nagata, A. Ogura, Ferroelectricity of $Hf_xZr_{1-x}O_2$ thin films fabricated by 300 °C low temperature process with plasma-enhanced atomic layer deposition, Microelectron. Eng. 215 (2019) 111013.
[23] S.J. Kim, J. Mohan, J. Lee, J.S. Lee, A.T. Lucero, C.D. Young, L. Colombo, S.R. Summerfelt, T. San, J. Kim, Effect of film thickness on the ferroelectric and dielectric properties of low-temperature (400 °C) $Hf_{0.5}Zr_{0.5}O_2$ films, Appl. Phys. Lett. 112 (2018) 172902.
[24] W.-Y. Liu, J.-J. Liao, J. Jiang, Y.-C. Zhou, Q. Chen, S.-T. Mo, Q. Yang, Q.-X. Peng, L.-M. Jiang, Highly stable performance of flexible $Hf_{0.6}Zr_{0.4}O_2$ ferroelectric thin films under multi-service conditions, J. Mater. Chem. C 8 (2020) 3878–3886.
[25] Y. Wei, S. Matzen, T. Maroutian, G. Agnus, M. Salverda, P. Nukala, Q. Chen, J. Ye, P. Lecoeur, B. Noheda, Magnetic tunnel junctions based on ferroelectric tunnel barriers, Phys. Rev. Appl. 12 (2019) 031001.
[26] M. Halter, L. Bégon-Lours, V. Bragaglia, M. Sousa, B.J. Offrein, S. Abel, M. Luisier, J. Fompeyrine, Back-end, CMOS-compatible ferroelectric field-effect transistor for synaptic weights, ACS Appl. Mater. Interfaces 12 (2020) 17725–17732.
[27] P.D. Lomenzo, C.-C. Chung, C. Zhou, J.L. Jones, T. Nishida, Doped $Hf_{0.5}Zr_{0.5}O_2$ for high efficiency integrated supercapacitors, Appl. Phys. Lett. 110 (2017) 232904.
[28] A. Chouprik, M. Spiridonov, S. Zarubin, R. Kirtaev, V. Mikheev, Y. Lebedinskii, S. Zakharchenko, D. Negrov, Wake-up in a $Hf_{0.5}Zr_{0.5}O_2$ film: a cycle-by-cycle emergence of the remnant polarization via the domain depinning and the vanishing of the anomalous polarization switching, ACS Appl. Electron. Mater. 1 (2019) 275–287.
[29] E.D. Grimley, T. Schenk, X. Sang, M. Pešić, U. Schroeder, T. Mikolajick, J.M. LeBeau, Structural changes underlying field-cycling phenomena in ferroelectric HfO_2 thin films, Adv. Eletron. Mater. 2 (2016) 1600173.
[30] D. Zhou, J. Xu, Q. Li, Y. Guan, F. Cao, X. Dong, J. Müller, T. Schenk, U. Schröder, Wake-up effects in Si-doped hafnium oxide ferroelectric thin films, Appl. Phys. Lett. 103 (2013) 192904.
[31] J. Bouaziz, P.R. Romeo, N. Baboux, B. Vilquin, Huge reduction of the wake-up effect in ferroelectric HZO thin films, ACS Appl. Electron. Mater. 1 (2019) 1740–1745.
[32] A. Kashir, S. Oh, H. Hwang, Defect engineering to achieve wake-up free HfO_2-based ferroelectrics, Adv. Eng. Mater. 23 (2021) 2000791.
[33] A. Kashir, H. Kim, S. Oh, H. Hwang, Large remnant polarization in a wake-up free $Hf_{0.5}Zr_{0.5}O_2$ ferroelectric film through bulk and interface engineering, ACS Appl. Electron. Mater. 3 (2021) 629–638.
[34] M.G. Kozodaev, A.G. Chernikova, E.V. Korostylev, M.H. Park, R.R. Khakimov, C.S. Hwang, A.M. Markeev, Mitigating wakeup effect and improving endurance of ferroelectric HfO_2-ZrO_2 thin films by careful La-doping, J. Appl. Phys. 125 (2019) 034101.
[35] K.-Y. Chen, P.-H. Chen, Y.-H. Wu, Excellent reliability of ferroelectric $HfZrO_x$ free from wake-up and fatigue effects by NH_3 plasma treatment, in: Symposium on VLSI Technology, 2017, pp. T84–T85.
[36] J. Lyu, I. Fina, R. Solanas, J. Fontcuberta, F. Sanchez, Robust ferroelectricity in epitaxial $Hf_{1/2}Zr_{1/2}O_2$ thin films, Appl. Phys. Lett. 113 (2018) 082902.
[37] J. Lyu, I. Fina, R. Solanas, J. Fontcuberta, F. Sanchez, Growth window of ferroelectric epitaxial $Hf_{0.5}Zr_{0.5}O_2$ thin films, ACS Appl. Electron. Mater. 1 (2019) 220–228.
[38] J. Lyu, I. Fina, F. Sanchez, Fatigue and retention in the growth window of ferroelectric $Hf_{0.5}Zr_{0.5}O_2$ thin films, Appl. Phys. Lett. 117 (2020) 072901.
[39] J. Lyu, T. Song, I. Fina, F. Sánchez, High polarization, endurance and retention in sub-5nm $Hf_{0.5}Zr_{0.5}O_2$ films, Nanoscale 12 (2020) 11280–11287.
[40] J. Lyu, I. Fina, J. Fontcuberta, F. Sanchez, Epitaxial integration on Si(001) of ferroelectric $Hf_{0.5}Zr_{0.5}O_2$ capacitors with high retention and endurance, ACS Appl. Mater. Interfaces 11 (2019) 6224–6229.
[41] T. Song, R. Bachelet, G. Saint-Girons, R. Solanas, I. Fina, F. Sánchez, Epitaxial ferroelectric La-Doped $Hf_{0.5}Zr_{0.5}O_2$ thin films, ACS Appl. Electron. Mater. 2 (2020) 3221–3232.
[42] Y. Wei, P. Nukala, M. Salverda, S. Matzen, H.J. Zhao, J. Momand, A.S. Everhardt, G. Agnus, G.R. Blake, P. Lecoeur, B.J. Kooi, J. Íñiguez, B. Dkhil, B. Noheda, A

rhombohedral ferroelectric phase in epitaxially strained $Hf_{0.5}Zr_{0.5}O_2$ thin films, Nat. Mater. 17 (2018) 1095–1100.

[43] P. Nukala, M. Ahmadi, J. Antoja-Lleonart, S. Graaf, Y. Wei, H.W. Zandbergen, B.J. Kooi, B. Noheda, In situ heating studies on temperature-induced phase transitions in epitaxial $Hf_{0.5}Zr_{0.5}O_2/La_{0.67}Sr_{0.3}MnO_3$ heterostructures, Appl. Phys. Lett. 118 (2021) 062901.

[44] L. Bégon-Lours, M. Mulder, P. Nukala, S. de Graaf, Y. Birkhölzer, B. Kooi, B. Noheda, G. Koster, G. Rijnders, Stabilization of phase-pure rhombohedral $HfZrO_4$ in pulsed laser deposited thin films, Phys. Rev. Mater. 4 (2020) 043401.

[45] P. Nukala, J. Antoja-Lleonart, Y. Wei, L. Yedra, B. Dkhil, B. Noheda, Direct epitaxial growth of polar (1−x)</number>HfO_2–(x)ZrO_2 ultrathin films on silicon, ACS Appl. Electron. Mater. 1 (2019) 2585–2593.

[46] P. Nukala, Y. Wei, V. Haas, Q. Guo, J. Antoja-Lleonart, B. Noheda, Guidelines for the stabilization of a polar rhombohedral phase in epitaxial $Hf_{0.5}Zr_{0.5}O_2$ thin films, Ferroelectrics 569 (2020) 148–163.

[47] J.P.B. Silva, R.F. Negrea, M.C. Istrate, S. Dutta, H. Aramberri, J. Íñiguez, F.G. Figueiras, C. Ghica, K.C. Sekhar, A.L. Kholkin, Wake-up free ferroelectric rhombohedral phase in epitaxially strained ZrO_2 thin films, ACS Appl. Mater. Interfaces 13 (2021) 51383–51392.

[48] A. El Boutaybi, T. Maroutian, L. Largeau, S. Matzen, P. Lecoeur, Stabilization by surface energy of the epitaxial rhombohedral ferroelectric phase in ZrO2. (2021) https://arxiv.org/abs/2111.05168.

[49] I. Fina, F. Sánchez, Epitaxial ferroelectric HfO_2 films: growth, properties, and devices, ACS Appl. Electron. Mater. 3 (4) (2021) 1530–1549.

[50] C. Liu, F. Liu, Q. Luo, P. Huang, X.X. Xu, H.B. Lv, Y.D. Zhao, X.Y. Liu, J.F. Kang, Role of oxygen vacancies in electric field cycling behaviors of ferroelectric hafnium oxide, in: IEEE International Electron Devices Meeting (IEDM), 2018, pp. 376–379.

[51] S.J. Kim, J. Mohan, S.R. Summerfelt, J. Kim, Ferroelectric $Hf_{0.5}Zr_{0.5}O_2$ thin films: a review of recent advances, JOM 71 (2019) 246–255.

[52] M. Yadav, A. Kashir, S. Oh, R.D. Nikam, H. Kim, H. Jang, H. Hwang, High polarization and wake-up free ferroelectric characteristics in ultrathin $Hf_{0.5}Zr_{0.5}O_2$ devices by control of oxygen-deficient layer, Nanotechnology 33 (2022) 085206.

[53] F.P.G. Fengler, M. Hoffmann, S. Slesazeck, T. Mikolajick, U. Schroeder, On the relationship between field cycling and imprint in ferroelectric $Hf_{0.5}Zr_{0.5}O_2$, J. Appl. Phys. 123 (2018) 204101.

[54] P. Nukala, M. Ahmadi, Y. Wei, S. de Graaf, E. Stylianidis, T. Chakrabortty, S. Matzen, H.W. Zandbergen, A. Björling, D. Mannix, D. Carbone, B. Kooi, B. Noheda, Reversible oxygen migration and phase transitions in hafnia-based ferroelectric devices, Science 372 (2021) 630–635.

[55] M. Zheng, Z. Yin, Y. Cheng, X. Zhang, J. Wu, J. Qi, Stabilization of thick, rhombohedral $Hf_{0.5}Zr_{0.5}O_2$ epilayer on c-plane ZnO, Appl. Phys. Lett. 119 (2021) 172904.

[56] M.H. Park, Y.H. Lee, T. Mikolajick, U. Schroeder, C.S. Hwang, Review and perspective on ferroelectric HfO_2-based thin films for memory applications, MRS Communications 8 (2018) 795–808.

[57] J. Wei, L. Jiang, M. Huang, Y. Wu, S. Chen, Intrinsic defect limit to the growth of orthorhombic HfO_2 and (Hf,Zr)O_2 with strong ferroelectricity: first-principles insights, Adv. Funct. Mater. 31 (2021) 2104913.

[58] M.D. Glinchuk, A.N. Morozovska, A. Lukowiak, W. Stręk, M.V. Silibin, D.V. Karpinsky, Y. Kim, S.V. Kalinin, Possible electrochemical origin of ferroelectricity in HfO_2 thin films, J. Alloys Compds. 830 (2020) 153628.

[59] T. Shimizu, T. Yokouchi, T. Oikawa, T. Shiraishi, T. Kiguchi, A. Akama, T.J. Konno, A. Gruverman, H. Funakubo, Contribution of oxygen vacancies to the ferroelectric behavior of $Hf_{0.5}Zr_{0.5}O_2$ thin films, Appl. Phys. Lett. 106 (2015) 112904.

[60] D.R. Islamov, T.M. Zalyalov, O.M. Orlov, V.A. Gritsenko, G.Y. Krasnikov, Impact of oxygen vacancy on the ferroelectric properties of lanthanum-doped hafnium oxide, Appl. Phys. Lett. 117 (2020) 162901.

[61] Y. Zhang, Q. Yang, L. Tao, E.Y. Tsymbal, V. Alexandrov, Effects of strain and film thickness on the stability of the rhombohedral phase of HfO_2, Phys. Rev Appl. 14 (2020) 014068.

[62] R. He, H. Wu, S. Liu, H. Liu, Z. Zhong, Ferroelectric structural transition in hafnium oxide induced by charged oxygen vacancies, Phys. Rev. B 104 (2021) L180102.

[63] D.H. Lee, Y. Lee, K. Yang, J.Y. Park, S.H. Kim, P.R.S. Reddy, M. Materano, H. Mulaosmanovic, T. Mikolajick, J.L. Jones, U. Schroeder, M.H. Park, Domains and domain dynamics in fluoritestructured ferroelectrics, Appl. Phys. Rev. 8 (2021) 021312.

[64] J.P.B. Silva, K.C. Sekhar, H. Pan, J.L. MacManus-Driscoll, Mário Pereira, Advances in dielectric thin films for energy storage applications, revealing the promise of group IV binary oxides, ACS Energy Lett. 6 (2021) 2208–2217.

[65] B. Max, M. Hoffmann, H. Mulaosmanovic, S. Slesazeck, T. Mikolajick, Hafnia-based double-layer ferroelectric tunnel junctions as artificial synapses for neuromorphic computing, ACS Appl. Electron. Mater. 2 (2020) 4023–4033.

[66] S. Dutta, P. Buragohain, S. Glinsek, C. Richter, H. Aramberri, H. Lu, U. Schroeder, E. Defay, A. Gruverman, J. Íñiguez, Piezoelectricity in hafnia, Nat. Commun. 12 (2021) 7301.